

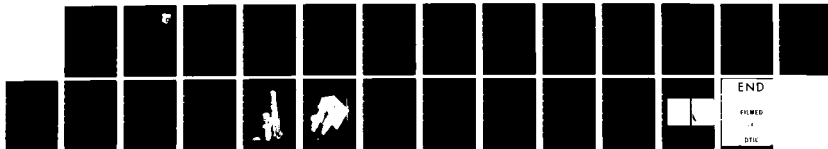
AD-A124 764

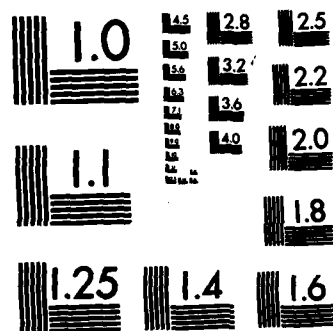
EFFECTS OF SURFACE CONDITIONS ON CARRIER TRANSPORT IN
III-V COMPOUNDS.: (U) ROCKWELL INTERNATIONAL THOUSAND
OAKS CA ELECTRONICS RESEARCH C. S P KOWALCZYK ET AL.
AUG 80 ERC41012. 67IP AFWAL-TR-80-1129 F/G 7/4

1/1

UNCLASSIFIED

NL

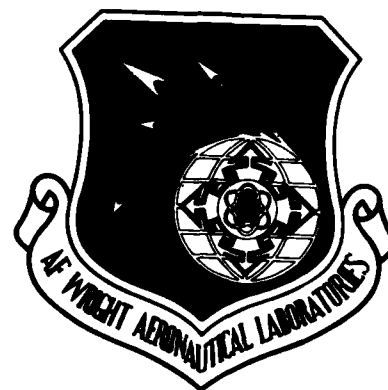




MICROCOPY RESOLUTION TEST CHART
NATIONAL BUREAU OF STANDARDS-1963-A

AFWAL-TR-80-1129

**EFFECTS OF SURFACE CONDITIONS ON
CARRIER TRANSPORT IN III-V COMPOUNDS**



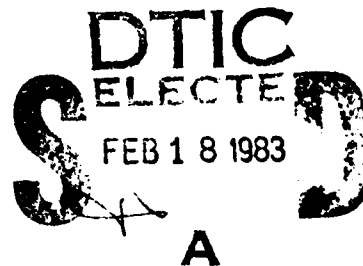
S. P. Kowalczyk, J. R. Waldrop, R. W. Grant, and W. A. Hill
Rockwell International Corporation
Electronics Research Center
1049 Camino Dos Rios
Thousand Oaks, California 91360

August 1980

Interim Report #3 for the Period
September 1, 1979 through March 1, 1980

Approved for public release; distribution unlimited.

AVIONICS LABORATORY
Air Force Wright Aeronautical Laboratories
Air Force Systems Command
Wright-Patterson Air Force Base, Ohio 45433



AD A124864

DTIC FILE COPY

NOTICE

When Government drawings, specifications, or other data are used for any purpose other than in connection with a definitely related Government procurement operation, the United States Government thereby incurs no responsibility nor any obligation whatsoever; and the fact that the government may have formulated, furnished, or in any way supplied the said drawings, specifications, or other data, is not to be regarded by implication or otherwise as in any manner licensing the holder or any other person or corporation, or conveying any rights or permission to manufacture, use, or sell any patented invention that may in any way be related thereto.

This report has been reviewed by the Information Office (OI) and is releasable to the National Technical Information Service (NTIS). At NTIS, it will be available to the general public, including foreign nations.

This technical report has been reviewed and is approved for publication.

Dietrich W. Langer

DIETRICH W. LANGER
Project Engineer
Electronic Research Branch
Avionics Laboratory

FOR THE COMMANDER

Philip E. Stover

PHILIP E. STOVER, Chief
Electronic Research Branch
Avionics Laboratory

"If your address has changed, if you wish to be removed from our mailing list, or if the addressee is no longer employed by your organization please notify AFWAL/AADR, W-PAFB, OH 45433 to help us maintain a current mailing list".

Copies of this report should not be returned unless return is required by security considerations, contractual obligations, or notice on a specific document.

Unclassified

SECURITY CLASSIFICATION OF THIS PAGE (When Data Entered)

REPORT DOCUMENTATION PAGE		READ INSTRUCTIONS BEFORE COMPLETING FORM
1. REPORT NUMBER AFWAL-TR-80-1129	2. GOVT ACCESSION NO. AD A734764	3. RECIPIENT'S CATALOG NUMBER
4. TITLE (and Subtitle) Effects of Surface Conditions on Carrier Transport in III-V Compounds		5. TYPE OF REPORT & PERIOD COVERED Interim Report #3 09/01/79 through 03/01/80
		6. PERFORMING ORG. REPORT NUMBER ERC41012.671P
7. AUTHOR(s) S. P. Kowalczyk, J. R. Waldrop, R. W. Grant, and W. A. Hill		8. CONTRACT OR GRANT NUMBER(s) F33615-78-C-1532
9. PERFORMING ORGANIZATION NAME AND ADDRESS Rockwell International Electronics Research Center 1049 Camino Dos Rios Thousand Oaks, CA 91360		10. PROGRAM ELEMENT, PROJECT, TASK AREA & WORK UNIT NUMBERS 2306/R1/80
11. CONTROLLING OFFICE NAME AND ADDRESS AFWAL/AADR Wright-Patterson Air Force Base, Ohio 45433		12. REPORT DATE August 1980
14. MONITORING AGENCY NAME & ADDRESS (if different from Controlling Office)		13. NUMBER OF PAGES 23
		15. SECURITY CLASS. (of this report) Unclassified
		15a. DECLASSIFICATION/DOWNGRADING SCHEDULE
16. DISTRIBUTION STATEMENT (of this Report) Approved for public release; distribution unlimited.		
17. DISTRIBUTION STATEMENT (of the abstract entered in Block 20, if different from Report)		
18. SUPPLEMENTARY NOTES		
19. KEY WORDS (Continue on reverse side if necessary and identify by block number) XPS, GaAs, surface chemistry, band bending, surface potential, oxidation		
20. ABSTRACT (Continue on reverse side if necessary and identify by block number) XPS (X-ray photoemission spectroscopy) measurements of surface chemistry and potential on vapor phase epitaxially grown n-type GaAs(100) and p-type bulk GaAs material are reported. Comparison of surface chemistry and potential is presented for bulk n- and p-type GaAs(100) samples. The assembly of several initial components of the contactless C-V apparatus is also described.		

Unclassified

SECURITY CLASSIFICATION OF THIS PAGE (When Data Entered)

TABLE OF CONTENTS

	Page
I. INTRODUCTION.....	1
II. XPS SURFACE STUDIES OF GaAs(100).....	3
1. Oxidation and Thermal Treatments of VPE Grown n-Type GaAs(100) Layer.....	3
2. Oxidation of Bulk p-Type GaAs(100).....	5
3. Comparison of Surface Band Bending on n- and p-Type GaAs(100) Surfaces.....	6
III. CONTACTLESS C-V APPARATUS.....	10
1. Assembly of Mechanical Components.....	10
2. Instrumentation of C-V Apparatus.....	14
3. Probe Tip Construction.....	18



Accession For	
NTIS GRA&I	<input checked="" type="checkbox"/>
DTIC TAB	<input type="checkbox"/>
Unannounced	<input type="checkbox"/>
Justification	
By _____	
Distribution /	
Availability	
Acquisition	
Date	
Signature	

A

LIST OF ILLUSTRATIONS

<u>Figure</u>		<u>Page</u>
1.	As 3d Binding Energy as Determined by XPS for n- and p-type GaAs(100) Samples.....	8
2.	Schematic Drawing Which Shows Relationship of z and θ Motion Components.....	11
3.	Assembled θ - Motion (Upper) and z - Motion (Lower) Components.....	12
4.	Gimbled Table With Motor-Driven Differential Screws. θ -Motion Assembly Shown in Fig. 3 Mounts in the Tube Which is Attached to the Gimbles.....	13
5.	Instrumentation of Contactless C-V Apparatus.....	15
6.	Contactless C-V Measurement Scheme.....	17
7.	Photograph of a Probe Tip Fabricated From a Highly Doped Silicon Wafer.....	19

I. INTRODUCTION

This is the third Interim Report for Contract No. F33615-78-C-1532 which is entitled "Effects of Surface Conditions on Carrier Transport in III-V Compounds." A goal of this program is to relate GaAs surface composition to surface electrical characteristics and to identify a surface treatment which provides stable, controllable, and reproducible chemical- and electrical-properties. High frequency microwave technology utilizes small dimension devices which places great importance on surface-potential stability and control of the surface potential in the active layer. Also, a useful GaAs MIS technology requires the development of an insulator/GaAs interface which has a sufficiently low interface state density so that inversion or accumulation can be obtained; such an interface could have considerable impact on future GaAs device technology.

The approach being followed in this program to correlate surface chemistry and potential makes use of x-ray photoemission spectroscopy (XPS) as discussed in the previous two interim reports. With this technique surface chemistry and composition, surface band bending and thus surface charge can be determined. A contactless C-V and G-V technique is also being developed as a supplementary probe of electrical interface properties. If successful, this technique should permit the determination of interface-state densities which, when coupled with the XPS measurements of surface chemistry, could allow information concerning the atomic nature of surface states to be obtained. A

contactless probe could also facilitate the correlation of transport measurements and surface composition.

The primary activity during the third six month phase of this program involved XPS studies of VPE (vapor phase epitaxy) grown n-type and bulk p-type GaAs(100) samples (Section II). In Section II.1 the studies on the VPE material are described, Section II.2 discusses studies on the p-type material and Section II.3 compares XPS surface potential and chemistry measurements for bulk n- and p-type GaAs(100) samples. Section III describes construction of the contactless C-V apparatus. The assembly of several of the initial mechanical components is outlined in Section III.1, instrumentation associated with control of the apparatus is discussed in Section III.2 and fabrication of the C-V probe tips is reported in Section III.3.

II. XPS SURFACE STUDIES OF GaAs(100)

Our previous XPS studies (see Interim Report #2) have concentrated on bulk, n-type GaAs (Crystal Specialties, boule #3686, $2 \times 10^{17} \text{ cm}^{-3}$ Te doped). In this section, initial studies of VPE samples (grown by the microwave section of ERC (Thousand Oaks), n-type, $4 \times 10^{16} \text{ cm}^{-3}$) and bulk p-type ($2 \times 10^{16} \text{ cm}^{-3}$) Crystal Specialties specimens are reported. Also, a comparative study of band bending on bulk (100) n- and p- surfaces is reported. Sample preparations and application of XPS for the determination of surface (or interface) potentials were described in detail in the last Interim Report (#2) and will not be repeated here.

1. Oxidation and Thermal Treatments of VPE Grown n-Type GaAs(100) Layer

The experiments reported in this section were carried out to determine if there were any significant differences in the chemistry and (interfacial) surface potential for VPE samples as compared to previously investigated bulk n-type GaAs. The results of various treatments are listed in Table 1. The VPE layer results are very similar to the earlier bulk results. The thermal treatments to about $\sim 690^\circ\text{C}$ * results in converting a surface with mixed Ga- and As- oxides to one of solely Ga_2O_3 . Further heat treatment at 710°C removes the Ga_2O_3 from the surface and results in a clean GaAs(100)

*The exact surface temperature is difficult to determine. The relative measured temperatures indicated throughout this report are all too high perhaps as much as $\sim 20\%$.

surface with a characteristic LEED pattern. Exposure of this clean surface to O_2 at elevated temperatures ($\sim 600^\circ C$) results in Ga_2O_3 formation and concomitant loss of the LEED pattern. These surface treatments result in a variation of the surface potential which closely mimics that observed for the surfaces of bulk samples. Namely, the Ga_2O_3 surface exhibits only a small band bending (~ 0.2 eV), while thermal cleaning results in a large band bending. Table 1 also summarizes results from the deposition of As (a heated quartz ampoule filled with GaAs was employed as an As source) on clean GaAs(100) at low substrate temperatures. Such depositions resulted in elemental As overlayers as detected by a 0.3 eV chemical shift of the As 3d line to higher binding energy; however, no change in surface potential was observed. Thermal treatment resulted in the As being easily driven off.

TABLE 1

XPS RESULTS FOR SEVERAL TREATMENTS OF GaAs(100) VPE #1100
($n = 4 \times 10^{16} \text{ cm}^{-3}$, $3\mu \text{ ON } n^+$) SURFACE^a

Treatment	Relative As 3d Binding Energy in GaAs (eV)	Remarks
690°C	+0.2	Ga ₂ O ₃
16 Hrs Vacuum	+0.3	---
710°C	0.0	Clean, LEED
$2 \times 10^4 \text{ L H}_2\text{O}$ (600°C)	0.0	---
$2 \times 10^4 \text{ L O}_2$ (600°C)	+0.2	Ga ₂ O ₃
700°C	0.0	Clean, LEED Ga 3d/As 3d \approx 0.88
Deposit As ^o (25°C)	(+0.3) ^b	Ga 3d/As 3d \approx 0.02 (No Significant Shift in Ga 3d Line)
700°C	0.0	Clean, LEED Ga 3d/As 3d \approx 0.88
Deposit As ^o (75°C)	(+0.3) ^b	Ga 3d/As 3d \approx 0.42 (No Significant Shift in Ga 3d Line)

^a - \approx 0.1 eV Binding Energy Instability

^b - Chemical Shift Due to As^o

2. Oxidation of Bulk p-Type GaAs(100)

This section will report our initial investigation of bulk p-type GaAs(100) surfaces. These results are summarized in Table 2. The chemistry of the p-type surface is similar to that for n-type described above. Heat treatment at 600°C produces a surface of Ga₂O₃, while further treatment at 705°C yields a clean surface with a characteristic LEED pattern. High temperature (600°C) oxidation results in a Ga₂O₃ covered surface. The surface-potential behavior as a function of treatment is discussed further in the next

section where a comparison of n- and p-type samples is presented. Only two points will be mentioned here, namely, the potential variations are similar to those observed for n-type (see Table 1) and, secondly, as previously reported (Interim Report #2 Contract No. F33615-78-C-1532), vacuum storage (at $\sim 2 \times 10^{-9}$ torr, 16 hours) results in a potential shift.

TABLE 2
XPS RESULTS FOR OXIDATION OF GaAs(100)
(p - $2 \times 10^{16} \text{ cm}^{-3}$) SURFACE^a

Treatment	Relative As 3d Binding Energy In GaAs (eV)	Remarks
600°C	+0.3	Ga ₂ O ₃
705°C	0.0	Clean, LEED
O ₂ $2 \times 10^4 \text{ L}$ (600°C)	+0.2	Ga ₂ O ₃
16 Hrs Vacuum	+0.3	---
Sputter 1 keV Ar ⁺ Anneal 350°C	-0.1	No LEED (Small Ga ₂ O ₃)

^a - ~ 0.1 eV Binding Energy Instability

3. Comparison of Surface Band Bending on n- and p-Type GaAs(100)

Surfaces

To facilitate comparison of the chemistry and surface potential variations between n- and p-type GaAs(100), an n and p specimen were simultaneously given a chemical etch in the same solution and then mounted side by side on the same sample platen. Thus, both samples were exposed to the same chemical and thermal treatments. The results are shown in Fig. 1,

where binding energies are reported on an absolute scale which is referenced to a thick Au deposit ($\sim 100 \text{ \AA}$) (Au $4f_{7/2}$ binding energy = 84.00 eV).^{*} As can be seen in Fig. 1, except for some small subtle ($\sim 0.1 \text{ eV}$) differences, the surface potentials for n and p type GaAs(100), as monitored by the As 3d core-level binding energy, track together in a highly correlated manner as a function of surface treatment. It must be remembered, however, that when considering the band-bending potential, this behavior is opposite. For example, consider the clean surface; when exposed to $2 \times 10^4 \text{ L O}_2$ at 575°C , the As 3d core level shifts by 0.18 eV to higher binding energy for both n- and p-GaAs(100). However, in the case of n GaAs(100), this means the band bending is reduced by 0.18 eV, while in the case of p GaAs(100) the band bending is increased by 0.18 eV. Another interesting aspect of Fig. 1 is that the surfaces can be prepared with at least several different surface potentials. This result may be in contradiction to the recently proposed Universal Defect Model for surface Fermi level pinning^{**} which suggests a unique pinning position for the energy bands on n- and p-type samples. One final interesting observation concerns the effect of Au deposits on the surface. Before terminating the experiment with a thick Au deposit for a final absolute reference energy determination, intermediate amounts of Au were deposited. At first only a small submonolayer amount of Au was deposited. The Au $4f_{7/2}$ binding energy had a 0.29 eV difference between n- and p-type

^{*}F. R. McFeeley, S. Kowalczyk, L. Ley, R. A. Pollak and D. A. Shirley, Phys. Rev. B **7**, 5228 (1973).

^{**}W. E. Spicer, I. Lindau, P. Skeath, C. Y. Su, and Patrick Chye, Phys. Rev. Lett. **44**, 420 (1980).

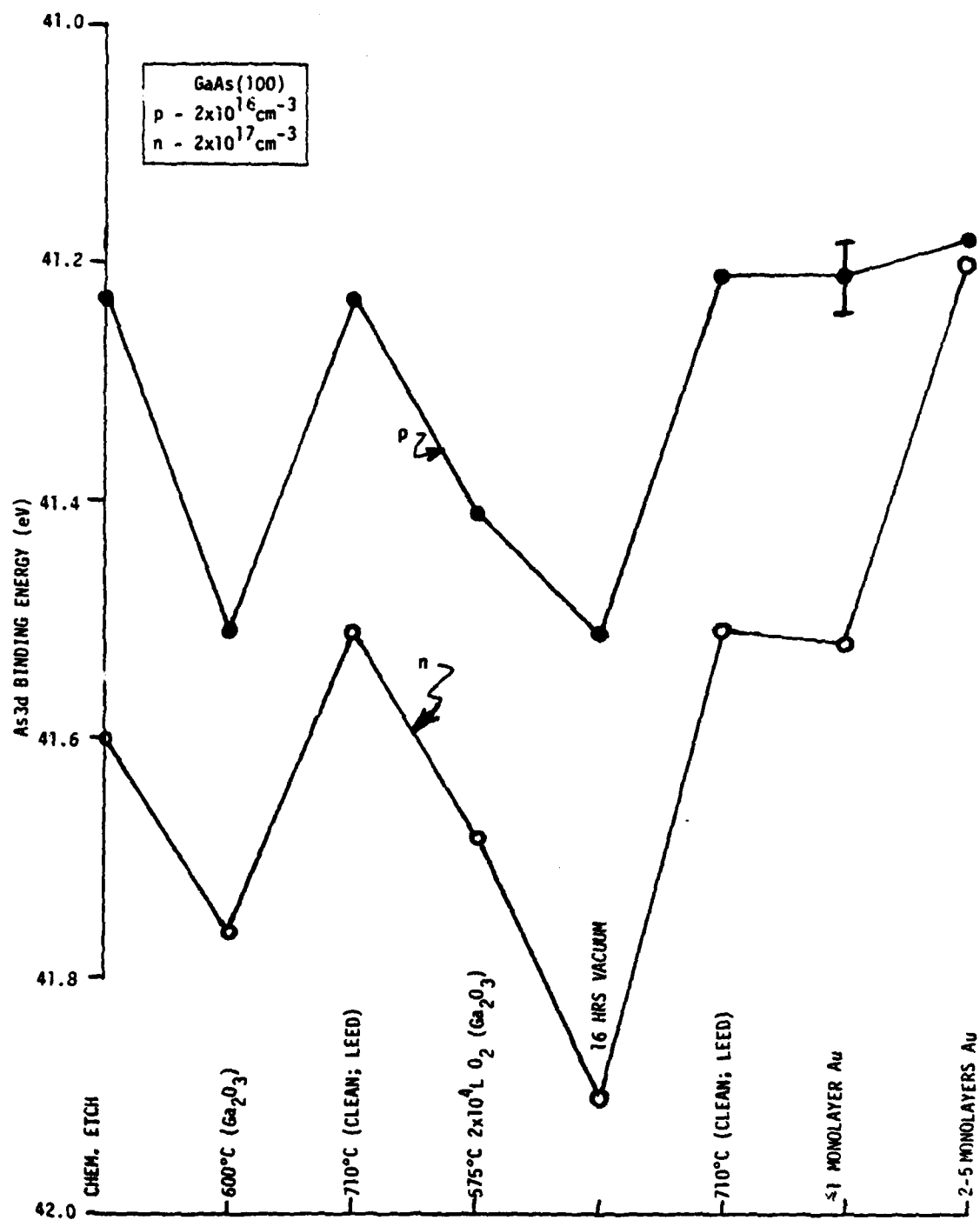


Fig. 1 As 3d Binding Energy as Determined by XPS for n- and p-type GaAs(100) Samples Subject to the Surface Treatments Indicated in the Figure.

GaAs, the same difference as observed for the As 3d binding energy in n and p GaAs. This submonolayer deposit had little effect on the surface potential as seen in Fig. 1. Next, the Au deposit was increased to several monolayers. At this point the Au 4f_{7/2} binding energy on n-GaAs decreased by 0.82 eV, while on the p-GaAs the Au 4f_{7/2} binding energy decreased by 0.53 eV. Now the Au 4f_{7/2} binding energy was the same on both n and p GaAs, i.e., 84.20 eV. At this point, there is a large surface potential shift in the n-type sample, which resulted in the same As 3d binding energy for the n and p type samples (see Fig. 1). A final thick deposit of Au resulted in a further shift of the Au 4f_{7/2} by 0.20 eV to lower binding energy; it was observed that a small amount of As was present on top of the Au deposit.

III. CONTACTLESS C-V APPARATUS

In this section, we describe the progress in construction and implementation of our proposed contactless C-V apparatus. The basic objective is to bring a 50 mil diameter circular probe to within a ~ 500 Å air gap of the surface of a GaAs sample to achieve a contactless C-V measurement. Section III.1 details the now completed assembly of several mechanical components of the apparatus and Section III.2 describes the design of the computerized electronic instrumentation. The fabrication of a highly flat probe tip is described in Section III.3

1. Assembly of Mechanical Components

Figure 2 is a crosssection view showing the relationship between the sample, the θ -motion assembly, and the Z-motion assembly. The GaAs sample is mounted on the end plate of the θ -motion transducer assembly (θ -TA), which in turn is attached to the gimble table (the reader is referred to Interim Reports 1 and 2, Contract No. F33615-78-C-1532, for additional details of the mechanical design). The upper part in Fig. 3 is the completed θ -TA, shown attached to a differential micrometer screw. When the θ -TA is mounted on the Gimble Table, this differential screw is adjusted manually to bring the top of the sample into the plane of the gimble pivots. The θ -TA consists of four ceramic piezoelectric transducer (CPT) pillars connected electrically so that opposing pairs can be activated to provide a tilt action. Figure 4 shows the completed Gimble Table Assembly in which the θ -TA will be mounted. The two

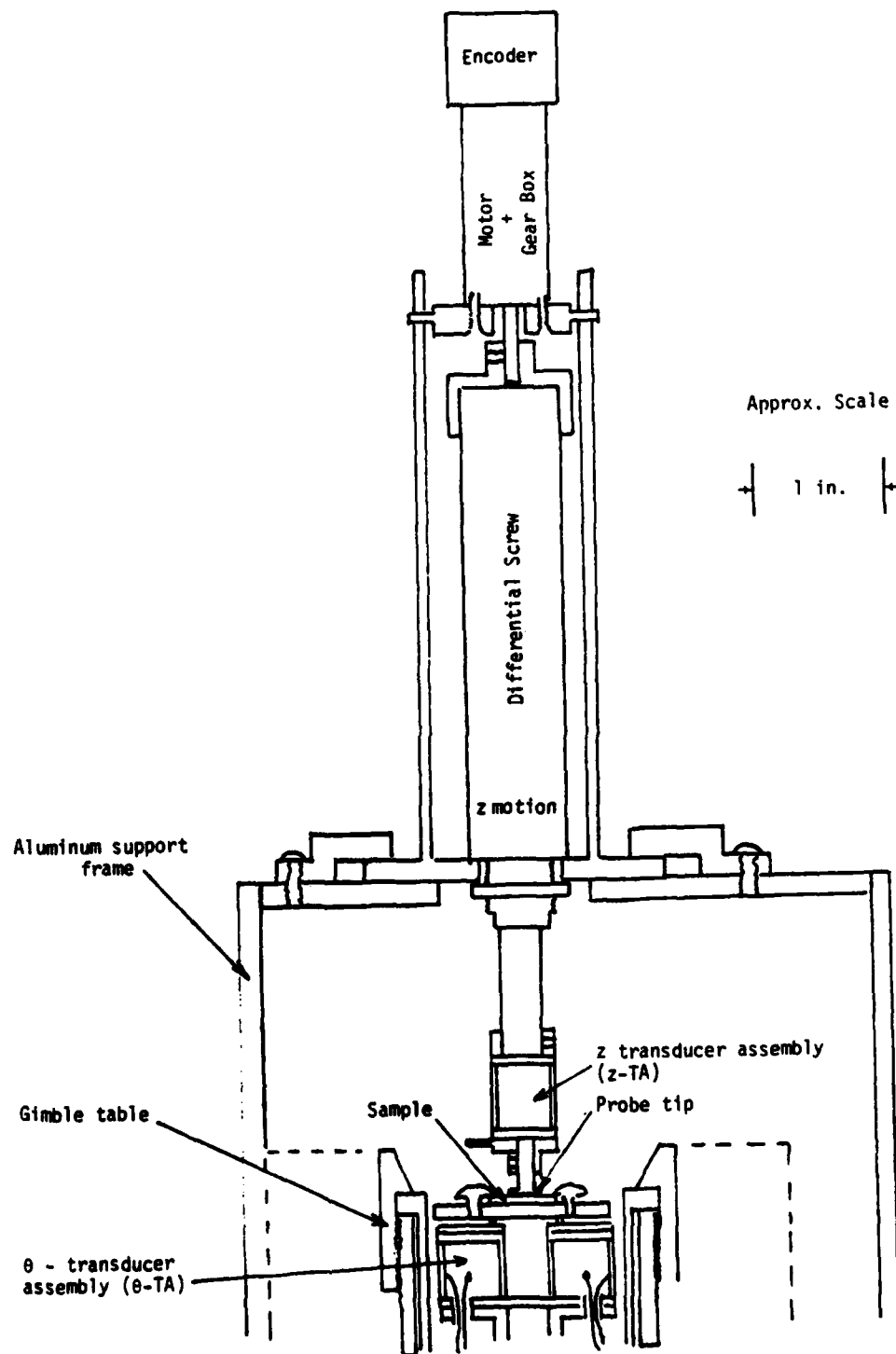


Fig. 2 Schematic Drawing Which Shows Relationship of z and θ Motion Components.

ERC80-8972



Fig. 3 Assembled θ - Motion (Upper) and z - Motion (Lower) Components.

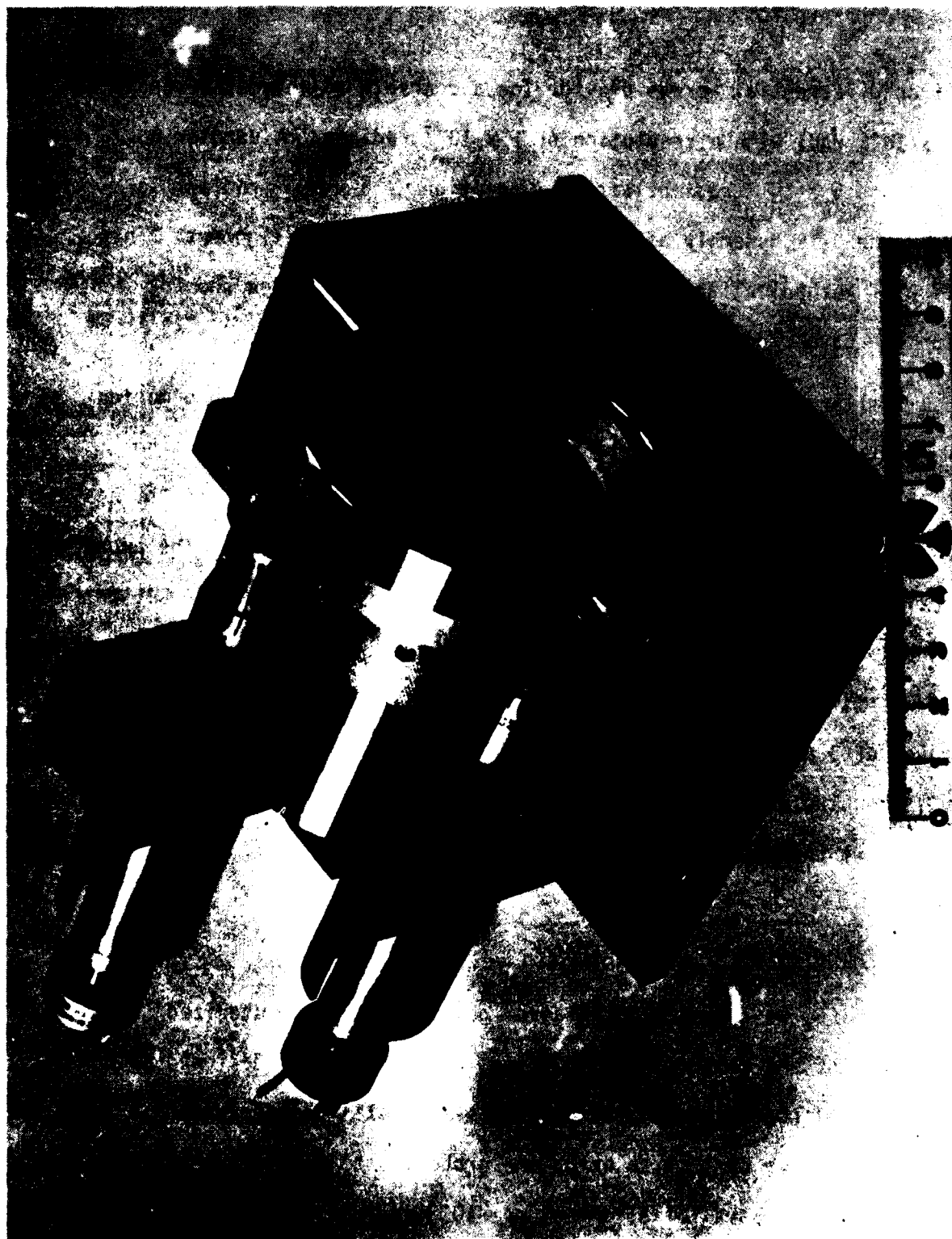


Fig. 4 Gimble Table With Motor-Driven Differential Screws.
 θ -Motion Assembly Shown in Fig. 3 Mounts in the Tube
 Which is Attached to the Gimbles.

motor-driven differential screws provide for a coarse θ adjustment of up to 2.5° (4×10^{-2} rad) with a resolution of 1×10^{-5} radians. A vernier θ motion of up to 5×10^{-4} radians with a resolution of 5×10^{-7} radians is provided by the θ -TA assembly after the coarse mechanical θ alignment. This combination of mechanical and electrical adjustment for θ motion should provide an adequate range for proper operation.

A similar coupling of mechanically- and electrically-induced motion was used for the gap spacing (z-motion) assembly. The completed z-motion assembly is shown in the lower half of Fig. 3. This assembly consists of a motor-driven differential screw to which is attached a CPT pillar. The probe tip (described in Section 3.3) is attached to the opposite end of the CPT to make up the Z-transducer assembly (Z-TA). The differential screw has a total motion of 10 mil (250 μ m) with a resolvable motion of 1000 \AA . The Z-TA has a total travel of 3 μ m with a resolvable motion of at least 50 \AA . The z-motion assembly is mounted directly over the θ -motion assembly by means of an aluminum support frame (Fig. 2).

2. Instrumentation of C-V Apparatus

In Fig. 5, we show a block diagram design of the computerized instrumentation of the contactless C-V system. The system is designed such that after initial coarse manual set-up, the system will operate under "closed-loop" computer control to bring the probe tip to within 500 \AA of the sample surface with a parallel alignment of $<10^{-6}$ radians.

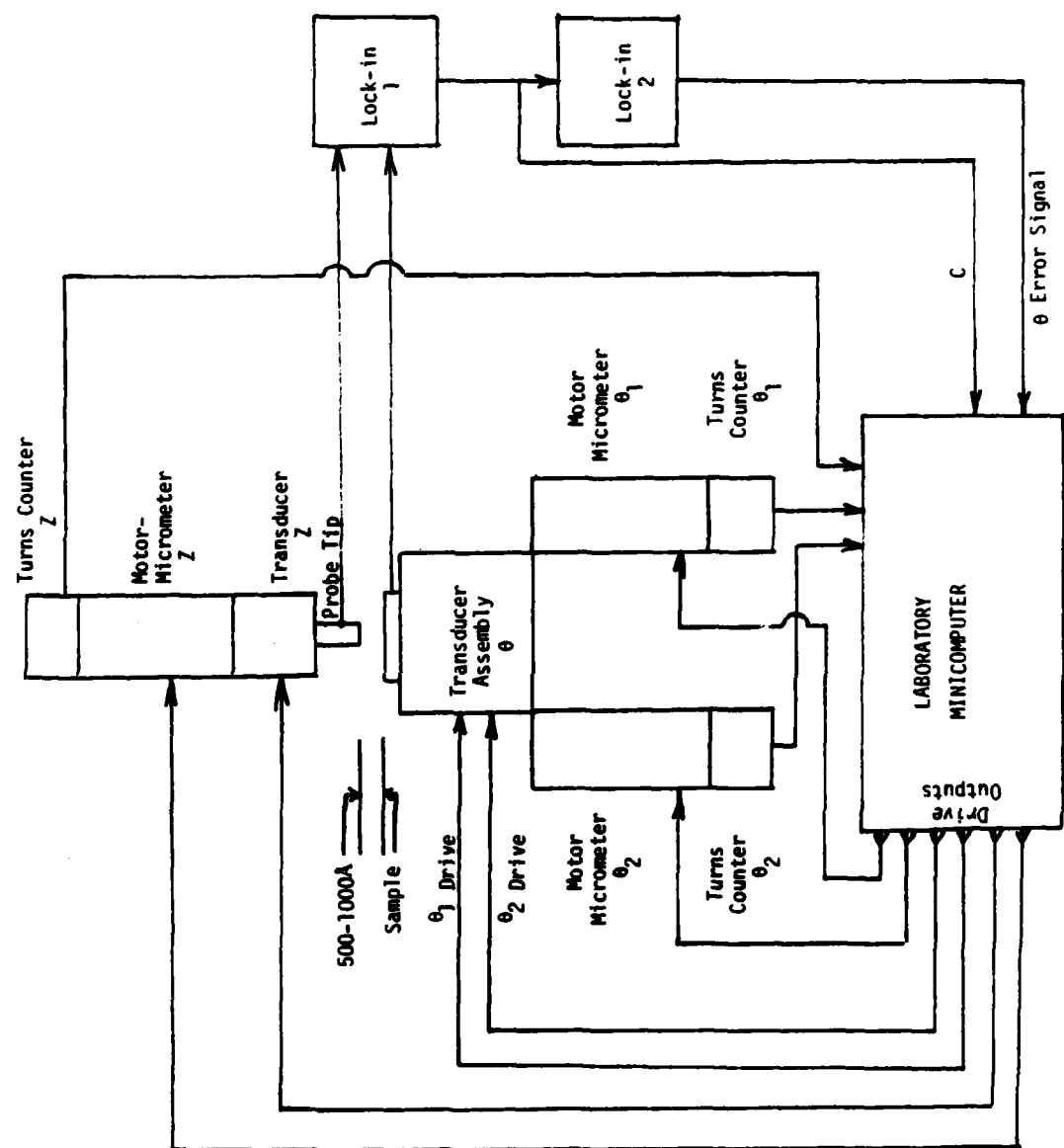


Fig. 5 Instrumentation of Contactless C-V Apparatus.

For clarity in explaining the operation of the system, we show in Fig. 6 the dual frequency modulation scheme derived in Interim Report #1 for detecting both the angular deviation from parallel, θ , between the probe and the sample and the spacing, d , between probe and sample. The gap spacing is measured by placing a small AC modulation voltage at frequency ω_v across the probe tip and sample. The angular deviation θ is modulated by applying a small AC voltage at frequency ω_c to the θ transducer assembly θ -TA ($\omega_v \gg \omega_c$). The output of lock-in 2 is thus an error signal for θ , θ_e , of $\theta_e \propto (\omega_v C_0 V_0 k \Delta \theta) \theta$, where the symbols are defined in Fig. 6. The output of lock-in 1 is a signal proportional to the capacitance, C , between the probe and sample, $C \propto \omega_v C_0 V_0 (1 + 2k \theta \Delta \theta \sin \omega_c t)$. Therefore, when $\theta = 0$, $C \propto \omega_v C_0 V_0$ and lock-in 1 measures $C_0 = \epsilon_0 A/d$, from which the gap spacing d is obtained.

In operation, the computer moves the z-motion drive until lock-in 1 gives a signal level which shows the probe is near the sample. The θ -alignment has two orthogonal degrees of freedom, θ_1 and θ_2 accomplished by the gimble table micrometers and the θ -TA. First, θ_1 is varied to minimize θ_e , then θ_2 is varied to produce $\theta_e = 0$. Output C then gives a measure of d . If d needs to be smaller the Z-micrometer or Z-TA can be used, followed by any necessary adjustment of θ_1 or θ_2 . To control the micrometers, the computer provides drive to the motors attached to the Z-micrometer differential screw and the θ_1 and θ_2 differential micrometer screws. Feedback to determine micrometer rotation is monitored by turn-counters attached to these motors, whose outputs are read by the computer. The drive for the Z-TA and θ -TA assemblies is a 0-1000 V signal also controlled by the computer. Feedback to

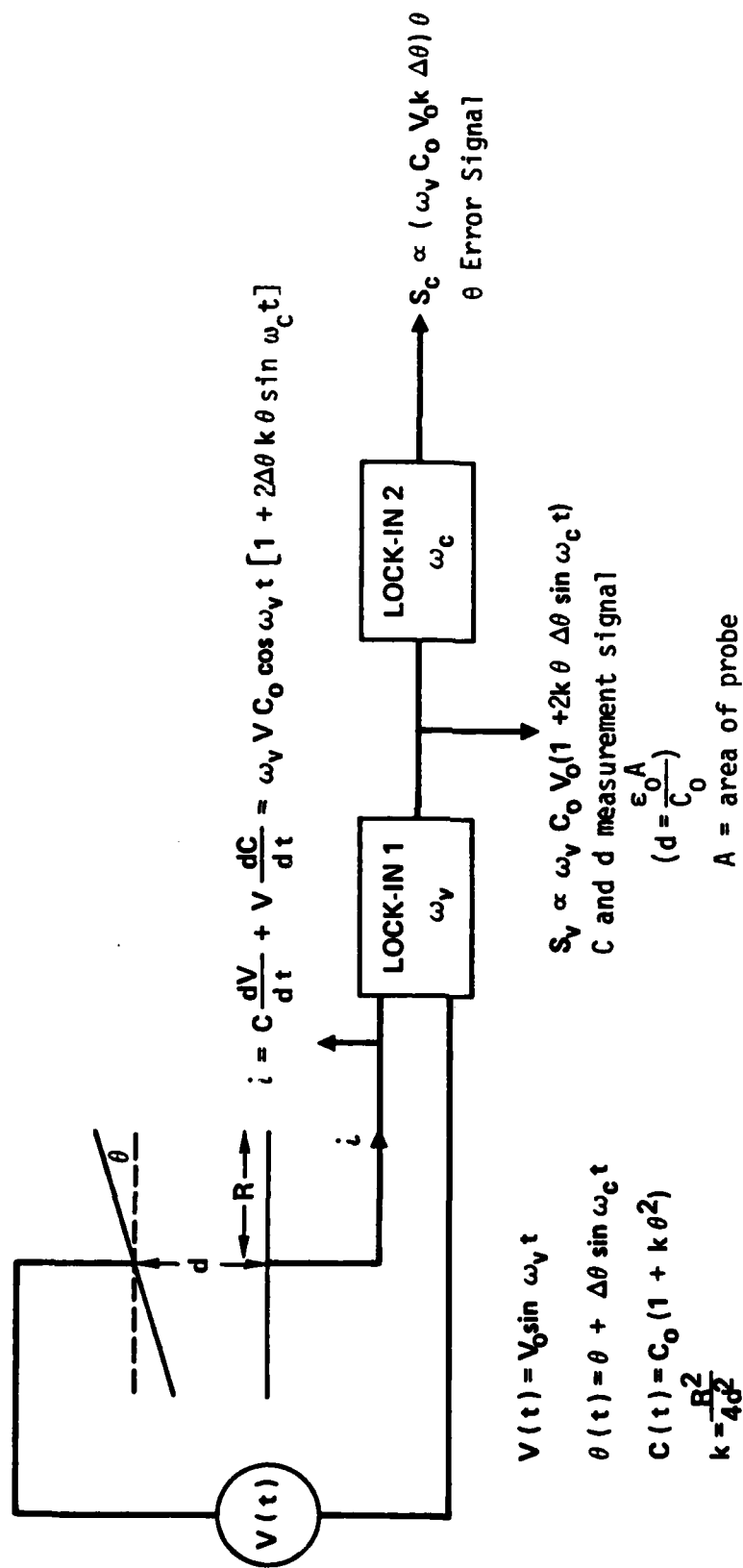


Fig. 6 Contactless C-V Measurement Scheme.

measure the effect of Z-TA and θ -TA changes is computer monitored by reading the output of lock-in 1 and lock-in 2, respectively. The Z-TA is designed so a 1V change in drive corresponds to a 50 Å change in d , the gap spacing. The θ -TA is designed such that a 1 V change in drive produces a 5×10^{-7} radian change in θ . This alignment sensitivity should be entirely adequate for proper operation of the C-V apparatus. We are presently in the initial stages of interfacing a computer (Analog Devices MacSym II) to the system.

3. Probe Tip Construction

Probe tips for the C-V apparatus have been fabricated as described below. First, degenerately doped Si ($\rho = 0.004$ ohm - cm) slices were sorted for flatness. It is necessary to maintain better than $0.5 \mu\text{m}$ surface variation per inch to achieve an acceptable probe tip flatness. The silicon wafers used exhibited less than $0.25 \mu\text{m}$ per inch surface variation in selected areas. Next, mesas were formed by isotropically etching the silicon from the top side; the backside of the wafers is thermally bonded to a glass slide with black wax. Liquified black wax was screened on to the smooth top surface of the wafer through an appropriate metal mask. The mask was lifted off and the wax was allowed to harden. This left a protective pattern of dots on the surface while the backside of the wafer was sealed and protected from the etch. The isotropic silicon etch solution used was nitric, acetic, and hydrofluoric acids ($\text{HNO}_3:\text{CH}_3\text{COOH}:\text{HF}$) in the proportions 7:2:1 respectively. This solution provides an etch rate of $\sim 5 \mu\text{m}$ per minute. The individual

mesas were then isolated by wafer sawing and each die was mounted on a metal carrier with either conductive epoxy or preform soldering. The final probe tip assembly is shown in Fig. 7.

ERC80-9033

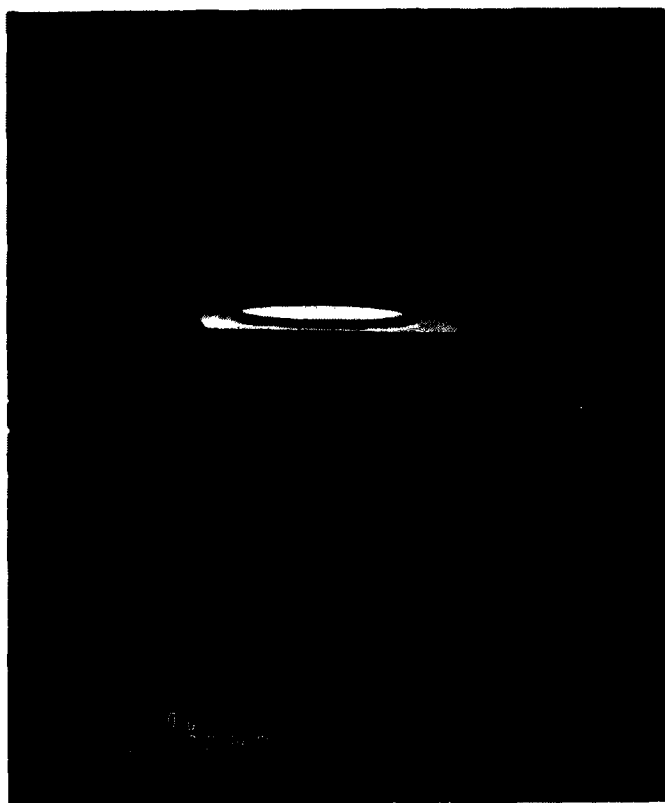


Fig. 7 Photograph of a Probe Tip Fabricated From a Highly Doped Silicon Wafer

END